Diabetologia (1997) 40: 1380–1387

Diabetologia

Originals

Localization in human diabetic peripheral nerve of Nε-carboxymethyllysine-protein adducts, an advanced glycation endproduct

K. Sugimoto[1, 2], **Y. Nishizawa**[1], **S. Horiuchi**[3], **S. Yagihashi**[1]

[1] Department of Pathology, Hirosaki University School of Medicine, Hirosaki, Japan
[2] Third Department of Internal Medicine, Hirosaki University School of Medicine, Hirosaki, Japan
[3] Department of Biochemistry, Kumamoto University School of Medicine, Kumamoto, Japan

Summary The present study was designed to elucidate in situ distribution of advanced glycation end-products (AGE) in human peripheral nerve and whether the reaction products were excessive in the diabetic condition. For the detection of AGE, immunoperoxidase staining was undertaken on peripheral nerve samples obtained from 5 non-insulin-dependent diabetic patients and 5 non-diabetic control subjects. The anti-AGE antibody used in this study contained an epitope against Nε-carboxymethyllysine. Light microscopically, AGE localized in the perineurium, endothelial cells and pericytes of endoneurial microvessels as well as myelinated and unmyelinated fibers. At the submicroscopic level, AGE deposition appeared focally as irregular aggregates in the cytoplasm of endothelial cells, pericytes, axoplasm and Schwann cells of both myelinated and unmyelinated fibers. Interstitial collagens, basement membranes of the perineurium also reacted with this antibody. The AGE depositions were detected in both control and diabetic nerves, but were more intense in the latter. The excessive AGE deposition correlated with a reduction in myelinated fiber density. However, the localization of AGE was not directly associated with degeneration of nerve fibers and the link between AGE deposition and nerve fiber degeneration is yet to be determined. The present study thus demonstrated the excessive deposition of intra- and extracellular AGE in human diabetic peripheral nerve and strengthened the contention that the enhanced glycation may play a role in the development of diabetic neuropathy. [Diabetologia (1997) 40: 1380–1387]

Keywords AGE, carboxymethyllysine, diabetes, peripheral nerve, neuropathy, immunohistochemistry, electron microscopy.

Amino groups of proteins non-enzymatically react with reducing sugars and form unstable adducts of Schiff bases, which reversibly convert to stable forms through Amadori rearrangement. Over time these reactions undergo further molecular modifications to yield irreversible crosslinking products of advanced glycation end-products (AGE). Long-lived proteins such as lens proteins [1, 2], basement membranes [3] and collagens [3–7] are prone to undergo AGE modification. The process is now considered to be implicated in aging and a variety of clinical disorders including Alzheimer's disease [8–10], atherosclerosis [11, 12] and diabetic complications [13–19].

It has been shown that the glycation process is exaggerated in diabetic peripheral nerve [20, 21]. In experimental diabetic animal models, inhibition of AGE formation with aminoguanidine was found to ameliorate functional and structural abnormalities of the peripheral nerve [13, 15, 19]. However, there is little information about which components of structural proteins in human diabetic peripheral nerve were modified with AGE. How AGE accumulation in these structural components is related to the pathological changes of diabetic neuropathy is still unclear. In the present study, we, therefore, examined

Received: 21 January 1997 and in revised form: 4 July 1997

Corresponding author: Dr. S. Yagihashi, First Department of Pathology, Hirosaki University School of Medicine, 5-Zaifucho, Hirosaki, Japan

Abbreviations: AGE, Advanced glycation end-products; PBS, phosphate buffered saline; BSA, bovine serum albumin; CML, carboxymethyllysine.

Table 1. Clinical characteristics of non-insulin dependent diabetic patients and non-diabetic control subjects examined in this study

	Biopsy/ autopsy	Cause of death	Age (years)	Sex	HbA_{1c} (%)	Duration of diabetes (years)	Treatment
Diabetic patients							
Case 1	biopsy	–	45	F	6.7	4	Insulin
Case 2	biopsy	–	57	M	9.1	27	Diet
Case 3	biopsy	–	73	F	7.2	22	Insulin
Case 4	autopsy	myeloblastoma	45	M	7.0	4	Insulin
Case 5	autopsy	cerebral infarct	77	M	6.5	< 1	Diet
Control subjects							
Case 6	biopsy	–	56	M	ND	–	–
Case 7	autopsy	dilated congestive cardiomyopathy	60	M	ND	–	–
Case 8	autopsy	superior mesenteric artery thrombosis	73	F	ND	–	–
Case 9	autopsy	colonic cancer	78	F	ND	–	–
Case 10	autopsy	acute myocardial infarct	79	M	ND	–	–

Non-diabetic control patients had blood glucose levels less than 6.1 mmol/l.
ND, not determined

in situ localization of AGE-modified proteins in peripheral nerve obtained by biopsy or at autopsy from diabetic patients by using a monoclonal antibody for Nε-carboxymethyllysine (CML), an AGE [1, 22]. We also performed histological examinations on these nerve samples and explored whether there is a relationship between AGE accumulation and clinicopathological changes. For comparison, peripheral nerves of non-diabetic subjects were examined.

Subjects and methods

Subjects. Ten peripheral nerve samples were obtained from 5 non-insulin-dependent diabetic patients and 5 non-diabetic control subjects. Clinical characteristics of the subjects in this study are summarized in Table 1. Nerve specimens were obtained by biopsy in 4 cases and at autopsy in the remaining 6 cases. Diagnosis and classification of diabetes were based on the criteria of the National Diabetes Data Group [23]. In the biopsy cases, 2 diabetic patients (cases 1 and 3) showed marked hyperglycaemia with elevated HbA_{1c} values (17.6 and 9.8 % at the time of admission) and suffered from severe pain in lower extremities. The pain continued for more than 6 months after the correction of hyperglycaemia with insulin treatment in both cases. Nerve biopsy was performed to examine whether diabetes-unrelated disorders such as vasculitis were underlying the chronic painful neuropathy. Case 2 presented with skin ulcers in the right toe and sole. Sural nerve sample was obtained when amputation was carried out on this patient. The other 2 diabetic patients (cases 4 and 5) had long-standing diabetes but died of non-diabetic causes lacking apparent neuropathic symptoms. The left sural nerves were taken at autopsy in these patients. The subjects used as non-diabetic controls had no history of diabetes and had fasting plasma glucose levels less than 6.1 mmol/l. In case 6 the right peroneal nerve was taken at the time of the leg operation and the saphenous nerve in the left leg was taken at the time of autopsy in case 10. In the biopsy cases, information including the nature, purpose, and potential risks of the operation was given before surgery to all the patients, who thereafter consented to the biopsy. Ethical committee approval was obtained from the Hirosaki University School of Medicine.

Tissue sampling and histological examinations. Peripheral nerve specimens 1–2 cm in length were obtained by total fascicular biopsy and at autopsy. The nerve specimens were fixed with 4 % paraformaldehyde in 0.1 mol/l phosphate buffer (pH 7.4) overnight and then cut into pieces of 3 mm in length. For morphological evaluation, a portion of the nerve sample in each case was postfixed with 1 % osmium tetroxide. After dehydration with graded series of ethanol, they were embedded in Epon 812 and polymerized. Semithin cross-sections of the nerve fascicle (1.0 μm in thickness) were obtained with an LKB Ultramicrotome (Bromma, Sweden) and subjected to light microscopic observations after staining with 1 % *p*-phenylenediamine.

Morphometric analyses of myelinated nerve fibers were performed on 1 % *p*-phenylenediamine-stained semithin cross-sections (1.0 μm) using a VIDAS image analysis system (Carl Zeiss, Tokyo) [24]. Myelinated fiber density was obtained by measurements of total myelinated fiber number divided by total fascicular area. When two or more nerve fascicles were observed, only the largest fascicle was used for the measurement. For the measurement of myelinated fiber diameter, we delineated the outer myelin border to obtain the fiber area, which was then converted to fiber diameter by assuming the area as a circle. More than 200 myelinated fibers were measured for this purpose in each case.

Immunohistochemistry. Immunohistochemical staining was performed by streptavidin biotin complex method [25, 26]. Briefly, after fixation with 4 % paraformaldehyde, nerve samples of 3 mm long were frozen in dry ice-cooled isopentane after cryoprotection by incubation with 1.5 and 2.3 mol/l sucrose in 0.1 mol/l phosphate buffer (pH 7.4) for 8 and 12 h at 4 °C, respectively. The frozen sections were obtained by a cryostat (Frigocut 2800 E, Reichert-Jung, Cambridge Instruments, Nußloch, Germany). At least 10 transverse sections, 40 μm thick in each case, were obtained. The sections were preincubated in a 0.3 % H_2O_2 solution in phosphate buffered saline (PBS) for 20 min at room temperature to inhibit background staining due to endogenous peroxidase activity. After washing with PBS for 10 min at least 6 times at 4 °C, the sections were

Table 2. Morphometric analysis of myelinated fibers of sural nerves of diabetic and non-diabetic control patients

	Nerve sample	Total fascicular area (mm^2)	Fiber number per fascicle	Fiber density ($\times 10^2/mm^2$)	Mean fiber diameter (μm)
Diabetic patients					
Case 1	sural	0.18	918	50.7	7.67
Case 2	sural	0.22	359	16.4	6.12
Case 3	sural	0.15	595	39.7	6.48
Case 4	sural	0.24	765	31.4	6.70
Case 5	sural	0.21	1359	65.7	6.87
Control subjects					
Case 6[a]	peroneal	0.06	–	–	–
Case 7	sural	0.20	2214	110.7	6.62
Case 8	sural	0.18	1409	77.4	6.85
Case 9	sural	0.17	1419	83.5	7.35
Case 10[a]	saphenous	0.05	–	–	–

[a] Morphometric analysis on myelinated fibers was not undertaken

incubated with 10 % normal rabbit serum (Histofine, Nichirei, Tokyo) for 2 h at room temperature to inhibit non-specific binding. The sections were then exposed to primary antibody (mouse monoclonal antibody for AGE) [1, 22] diluted to 1.0 μg/ml with PBS containing 1 % bovine serum albumin (BSA) and 0.1 % sodium azide for 48 h at 4 °C. After washing with PBS three times for 10 min, secondary antibody (rabbit biotinylated anti-mouse IgA + IgG + IgM antibody: Histofine) was added for 2 h at room temperature. The sections were then incubated with peroxidase-conjugated streptavidin for 2 h at room temperature. To visualize the immunoreactions, sections were incubated with diaminobenzidine (DAB) in PBS containing 0.025 % cobalt chloride, 0.02 % nickel ammonium sulfate, and 0.065 % sodium azide.

The procedure for the observation by a confocal laser scan microscope was the same as that described for application of the secondary antibody. It was followed by a rinse in PBS and incubation with fluorescein isothiocyanate (FITC)-labelled goat anti-rabbit IgG antibody for 16 h at 4 °C. The stained sections were observed by a laser scan microscope (LSM310; Carl Zeiss). The scanning conditions including contrast, brightness level and pinhole size were set constant throughout the whole observation period for both control and diabetic samples.

Immunoelectron microscopy. The sections stained with anti-AGE-BSA antibody were osmicated (1 % osmium tetroxide) in 0.1 mol/l phosphate buffer (pH7.4) and embedded in Epon 812. Ultrathin sections were obtained with a ultramicrotome and examined with a JEOL 2000 electron microscope (Nihon-Denshi, Tokyo, Japan) after staining with lead citrate for 5 min or without staining.

Negative control and specificity of primary antibody. Immunostainings for negative control were performed by replacing the primary antibody by normal mouse serum. For specificity of primary antibody, preincubation of the primary antibody with an excess amount of AGE-BSA for 1 h at room temperature was also carried out. Following these preparations, the sections were processed to immunostaining as described above and analysed together with the other sections without these pretreatment procedures.

Statistical analysis. All morphometric analyses and evaluation for intensity of immunoreactivity for AGE in each case were performed in a blinded manner. The significance of differences between the mean values of diabetic and non-diabetic control patients was analysed by Mann-Whitney U-test (StatView-J 4.11). Relationships between variables were assessed by calculating Pearsons' simple correlation coefficients. A p-value less than 0.05 was considered statistically significant.

Results

Histological examinations. By light microscopy diabetic patients showed apparent myelinated fiber loss in Cases 1, 2, 3 and 4 in which myelinated fiber density was reduced when comparing with that in non-diabetic nerves (Table 2). The remaining myelinated fibers underwent active fiber degeneration and myelin breakdown. Mean fiber diameter was not altered in diabetic nerves compared with non-diabetic nerves. Endoneurial microvessels of diabetic patients showed narrowed lumens and thickened walls. No vasculitic changes were detected. By contrast, there were no apparent fiber loss in non-diabetic nerve samples and only a few degenerative fibers were noted. Walls of endoneurial microvessels appeared to be thinner compared with those in diabetic nerves.

Immunohistochemistry. Immunohistochemical examination with light microscopy demonstrated that AGE was located in the perineurium, axons and Schwann cells of myelinated fibers, endothelial cells and pericytes of endoneurial microvessels both in diabetic and non-diabetic control nerves (Fig. 1). In addition, there were scattered positive reactions in areas of unmyelinated fibers in diabetic nerves. Such endoneurial reactions particularly of microvessels and perineurium were strong in diabetic nerves but obscure in non-diabetic nerves (Fig. 1). Occasionally, interstitial fibroblasts showed positive reactions. When the primary antibody was replaced by normal mouse serum or preincubated with AGE-BSA, both preparations showed diminished immunostaining. However, labellings were occasionally observed in the axons and Schwann cells of myelinated fibers, which may be

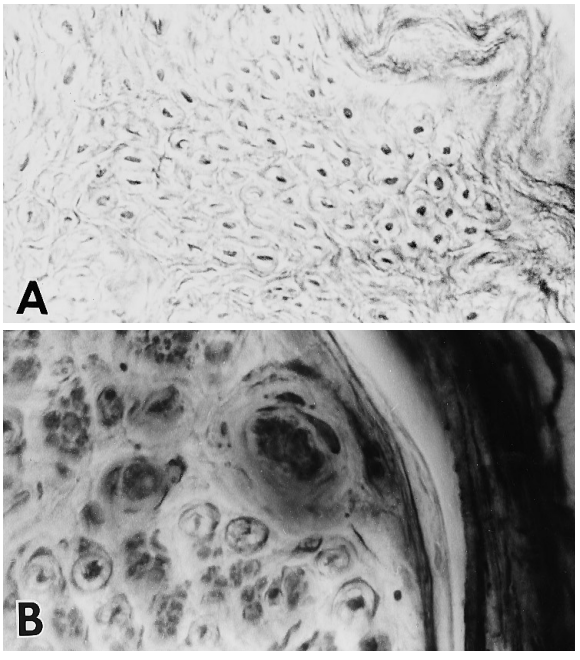

Fig. 1 A, B. Immunoperoxidase staining for AGE on peripheral nerves from a non-diabetic control subject (Case 6) (**A**) and a diabetic patient (Case 4) (**B**). **A**: Positive reactions to AGE in perineurium and axons of myelinated fibers. **B**: Diabetic nerves show strongly positive reactions in perineurium, endoneurial microvascular walls, axons of myelinated and unmyelinated fibers. (**A**: × 600, **B**: × 600)

non-specific reactions due to endogenous tissue peroxidase.

Results from immunofluorescence analysis with a confocal laser scan microscopy were comparable to those of immunoperoxidase staining (Fig. 2). AGE was distributed in the cytoplasm of Schwann cells, endothelial cells and pericytes. In addition, isolated oval or polygonal cells presumed to be macrophages were positive both in control and diabetic nerves. In contrast to immunoperoxidase staining, positive reactions were totally abolished when the primary antibody was replaced by normal mouse serum and when the sections were preincubated with AGE-BSA.

When the intensity of immunostaining signals was graded as –, none; ± , equivocal; + , weak; + + , moderate; + + + , strong, most of perineurial and endoneurial tissue components in diabetic nerves were scored as high grade (Table 3). Perineurial cells and myelinated axons in non-diabetic nerves also showed strong reactions, whereas differences in the staining intensities between diabetic and non-diabetic nerves were most conspicuous in endothelial cells and pericytes of endoneurial microvessels. When the graded intensity was numerically scored as –, 0; ± , 0.5; + , 1; + + , 2; and + + + , 3; the overall intensity as a total sum of each of the scores of tissue components was significantly increased in diabetic nerves as compared with non-diabetic control nerves ($p < 0.01$) (Fig. 3).

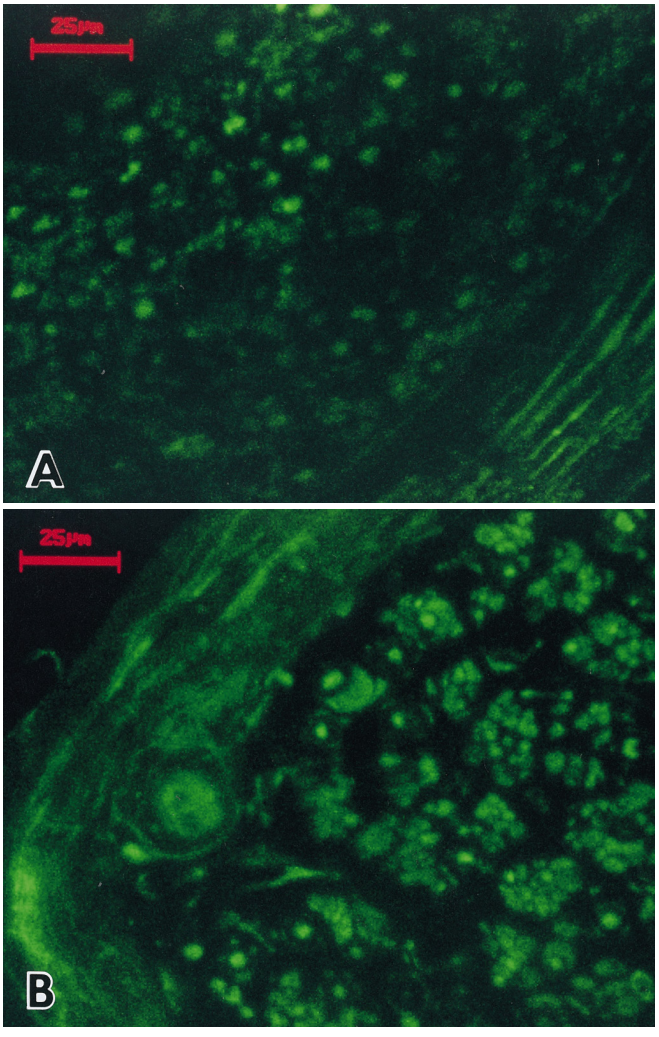

Fig. 2A, B. Confocal laser scan microscope pictures for AGE on peripheral nerves from non-diabetic control patient (**A**: Case 7) and a diabetic patient (**B**: Case 5). Localization of positive sites is comparable to Figure 3 in both diabetic and non-diabetic control patients, but the signals are intensified in diabetic nerve as compared with those in non-diabetic nerve

The overall intensity was not correlated with age or duration of diabetes, but there was a significant negative correlation between the overall intensity and myelinated fiber density (Fig. 4).

Immunoelectron microscopy. At the electron microscopic levels, positive reactions were depicted as irregular deposition of black peroxidase reactions. There were focally aggregated deposits both intra- and extracellularly. They located in the perineurial collagens, cytoplasm of perineurial cells and their basement membranes (Fig. 5A) as well as the cytoplasm of endothelial cells and pericytes of endoneurial microvessels (Fig. 5B). The axoplasm and cytoplasm of Schwann cells of both unmyelinated and myelinated fibers showed focally strong positive reactions (Fig. 5C, D). Fibroblasts and macrophages

Table 3. Semiquantitative analysis on the intensities of AGE immunoreactions at light microscopic levels in the peripheral nerve samples of diabetic and non-diabetic patients

	Perineurium		Endoneurial microvessels		Myelinated fibers		Unmyelinated fibers
	Perineurial cells	Collagens	Endothelial cells	Pericytes	Schwann cells	Axons	
Diabetic patients							
Case 1	+++	++	++	+	+	+	+
Case 2	+++	++	++	++	+	+	++
Case 3	+++	+++	+++	+++	++	+++	+++
Case 4	+++	++	+++	+++	++	+++	+++
Case 5	++	+	+++	++	++	++	+++
Control subjects							
Case 6	++	+	–	–	±	+++	±
Case 7	±	–	±	–	+	+	±
Case 8	++	+	±	±	±	+++	±
Case 9	+	+	±	–	±	+	+
Case 10	++	+	±	–	++	+++	++

–, negative; ±, equivocal; +, positive; ++, moderately positive; +++, strongly positive

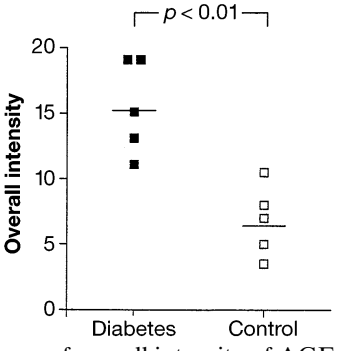

Fig. 3. The scores of overall intensity of AGE reactions in diabetic (■) and non-diabetic control patients (□) (see text). Average overall intensity is significantly increased in diabetic patients as compared with non-diabetic patients ($p < 0.01$). Bar indicates mean values in each group

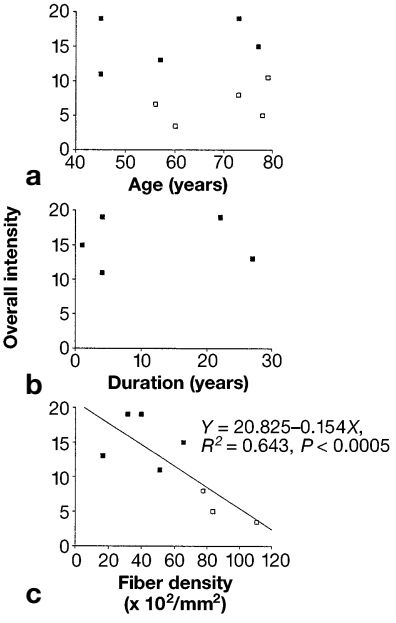

Fig. 4. Relationships between the intensity scores of AGE reactions and age (**a**), duration of diabetes (**b**) and myelinated fiber density (**c**). Scores of diabetic nerves ■; non-diabetic control nerves □. No significant correlation is detected between the intensity and age or duration of diabetes, whereas the inverse correlation with myelinated fiber density is significant ($p < 0.001$)

contained positive reaction products (data not shown).

Discussion

In the present study, we demonstrated the localization of immunoreactive AGE in the peripheral nerve of diabetic and non-diabetic patients. The reaction products were demonstrated both intra- and extracellularly in perineurial and endoneurial tissues as well as microvessels. The overall staining intensity was significantly increased in diabetic nerves compared with non-diabetic nerves, although strong reactions were also found in perineurial cells and axons of myelinated fibers in non-diabetic nerves. We could not detect an apparent age-related increase in AGE deposition. Peripheral nerve is thus likely to undergo excessive glycation in the diabetic condition as occurs in other diabetic tissues [27]. The current data has also shown that the overall intensity of AGE reactions correlated with myelinated fiber loss, implicating the role of the glycation process in the cause and development of diabetic neuropathy.

The primary monoclonal antibody used in this study was generated by using AGE-modified BSA as an immunogen in mice [22]. The major epitope of this antibody was recently found to be an Nε-(carboxymethyl)lysine(CML)-modified adduct [28]. Various AGE-modified proteins including peptides and lysine derivatives all reacted with this antibody [22]. These findings suggested that whatever the protein

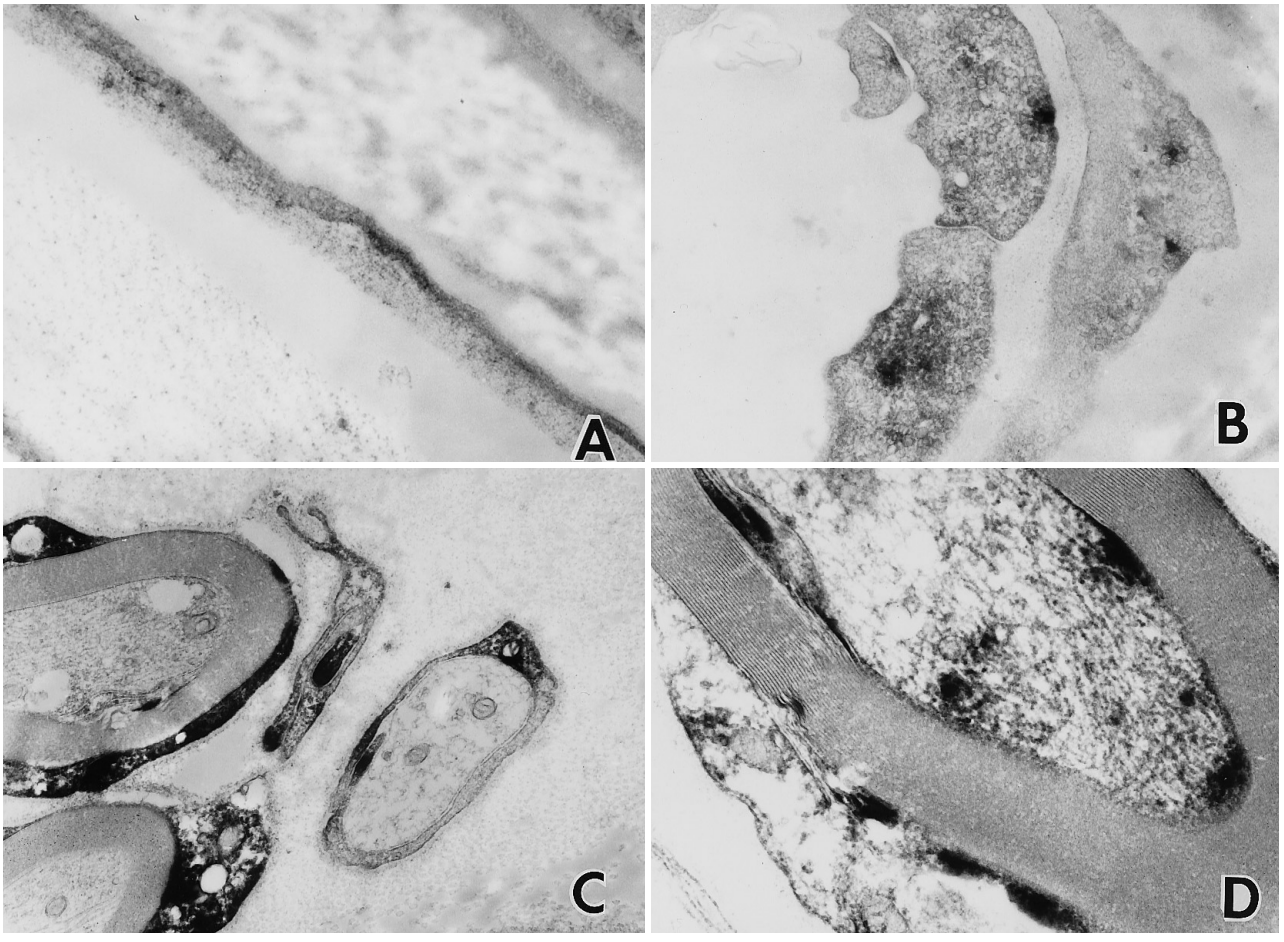

Fig. 5. Immunoelectron microscopy for AGE. **A**: Granular and patchy AGE depositions are localized in the cytoplasm of perineurial cells and the basement membranes as well as perineurial collagens (× 27,000). **B**: The cytoplasm of endothelial cells and pericytes of endoneurial microvessels is focally positive for AGE (× 22,000). **C**: AGE depositions are localized in the cytoplasm of Schwann cells of both myelinated and unmyelinated fibers (× 16,300). **D**: There are AGE depositions within the axoplasm of myelinated fibers (× 27,000)

is, common AGE products containing an epitope of CML are produced after progressive addition of glucose. Besides the modification of the Amadori products into CML with advancement of the glycation process, CML adducts of AGE are also formed by oxidative cleavage of the Amadori products at a relatively early stage of non-enzymatic glycation [29]. Intracellular as well as extracellular deposition of AGE detected in this study may therefore be the results of hyperglycaemia-induced in situ accumulation of glycation products or secondary products caused by oxidative stress. It remains unclear, however, whether other non-CML-type AGE may co-localize intracellularly or extracellularly with CML-type AGE or whether topographic distribution of CML is different from non-CML-type AGE.

In the present study, CML-type AGE was found in the cytoplasm of myelinated and unmyelinated fibers and endoneurial microvessels. Although overall reactions were intensified in diabetic nerve, the localization of AGE in nerve fibers did not appear to be directly associated with the pathologic processes of nerve fiber degeneration. These results do not necessarily undermine the significance of enhanced glycation in the pathogenesis of diabetic neuropathy when taking into consideration the biological action of AGE such as free radical formation, NO depletion and abnormal biological signalling [10, 30–32]. It is of note that perineurial cells and their basement membranes as well as perineurial collagens reacted with AGE. Perineurial cells and their basement membranes are thought to play a crucial role in the maintenance of perifascicular diffusion barrier to the macromolecules such as AGE-modified proteins [33, 34]. It may be possible that the excessive accumulation of AGE-modified adducts in the perineurium as well as endoneurial microvasculature alters the endoneurial microenvironment and microcirculation and thereby contributes to the development of peripheral neuropathy in diabetes.

Our ultrastructural examinations revealed that intracellular AGE did not have specific affinity with cytoplasmic organelles but rather distribute

non-randomly as electron dense aggregates. It has been shown that fractions of tubulin as well as neurofilament are glycated in the peripheral nerve of streptozotocin diabetic rats [35–37]. Preservation of axoplasmic tubulin and neurofilaments is sometimes difficult in immunoelectron microscopic preparations. Such methodological problems may have caused difficulty when identifying the susceptible organelles, but the diffuse aggregation of reaction products on the subcellular structures of microtubules as well as neurofilaments is in keeping with the previous findings of excessive glycation of tubulin and neurofilaments in nerve of diabetic animal models [35–37]. The glycation of such axonal components may result in the impairment of axonal flow and impaired impulse propagation and thereby functional and structural abnormalities.

In summary, we clearly demonstrated the in situ localization of AGE in the peripheral nerve, which was augmented in diabetic patients and associated with myelinated fiber loss. We could not find, however, a direct link between AGE deposition and pathological changes of nerve fibers. The number of the nerves examined in this study was too small to lead to any conclusion on the specific role of glycation in the pathogenesis of diabetic neuropathy. Further studies are warranted to elucidate the mechanisms by which the processes of AGE formation are involved in the pathogenesis of diabetic neuropathy.

Acknowledgements. The authors are greatly indebted to Dr. S. Toh, Department of Orthopedic Surgery, and Dr. M. Kaimori, Department of Pathology, Aomori Prefectural Hospital for their kind cooperation to complete this study. Technical assistance of Ms. M. Sugo is also appreciated.

References

1. Araki N, Ueno N, Chakrabarti B, Morino Y, Horiuchi S (1992) Immunochemical evidence for the presence of advanced glycation end products in human lens proteins and its positive correlation with aging. J Biol Chem 267: 10211–10214
2. Marion MS, Carlson EC (1994) Immunoelectron microscopic analyses of Maillard reaction products in bovine anterior lens capsule and Descemet's membrane. Biochim Biophys Acta 1191: 33–42
3. Brownlee M, Vlassara H, Kooney A, Ulrich P, Cerami A (1986) Aminoguanidine prevents diabetes-induced arterial wall protein cross-linking. Science 232: 1629–1632
4. Fu MX, Knecht KJ, Thorpe SR, Baynes JW (1992) Role of oxgen in cross-linking and chemical modification of collagen by glucose. Diabetes 41 [Suppl 2]:42–48
5. Fu MX, Wells-Knecht KJ, Blackledge JA, Lyons TJ, Thorpe SR, Baynes JW (1994) Glycation, glycosylation, and cross-linking of collagen by glucose. Kinetics, mechanisms, and inhibition of late stages of the Maillard reaction. Diabetes 43: 676–683
6. Monnier VM, Kohn RR, Cerami A (1984) Accelerated age-related browning of human collagen in diabetes mellitus. Proc Natl Acad Sci USA 81: 583–587
7. Monnier VM, Sell DR, Nagaraj RH et al. (1992) Maillard reaction-mediated molecular damage to extracellular matrix and other tissue proteins in diabetes, aging, and uremia. Diabetes 41[Suppl 2]:36–41
8. Smith MA, Taneda S, Richey PL et al. (1994) Advanced Maillard reaction end products are associated with Alzheimer disease pathology. Proc Natl Acad Sci USA 91: 5710–5714
9. Vitek MP, Bhattacharya K, Glendening JM et al. (1994) Advanced glycation end products contribute to amyloidosis in Alzheimer disease. Proc Natl Acad Sci USA 91: 4766–4770
10. Yan SD, Chen X, Schmidt AM et al. (1994) Glycated tau protein in Alzheimer disease: A mechanism for induction of oxidative stress. Proc Natl Acad Sci USA 91: 7787–7791
11. Kume S, Takeya M, Mori T et al. (1995) Immunohistochemical and ultrastructural detection of advanced glycation end products in atherosclerotic lesions of human aorta with a novel specific monoclonal antibody. Am J Pathol 147: 654–667
12. Nakamura Y, Horii Y, Nishino T et al. (1993) Immumohistochemical localization of advanced glycosylation end-products in coronary atheroma and cardiac tissue in diabetes mellitus. Am J Pathol 143: 1649–1656
13. Cameron NE, Cotter MA, Dines K, Love A (1992) Effects of aminoguanidine on peripheral nerve function and polyol pathway metabolites in streptozotocin-diabetic rats. Diabetologia 35: 946–950
14. Hammes H-P, Martin S, Federlin K, Geisen K, Brownlee M (1991) Aminoguanidine treatment inhibits the development of experimental diabetic retinopathy. Proc Natl Acad Sci USA 88: 11555–11558
15. Kihara M, Schmelzer JD, Poduslo JF, Curran GL, Nickander KK, Low PA (1991) Aminoguanidine effects on nerve blood flow, vascular permeability, electrophysiology, and oxygen free radicals. Proc Natl Acad Sci USA 88: 6107–6111
16. Makino H, Shikata K, Hironaka K et al. (1995) Ultrastructure of nonenzymatically glycated masangial matrix in diabetic nephropathy. Kidney Int 48: 517–526
17. Miyata S, Monnier V (1992) Immunohistochemical detection of advanced glycosylation end products in diabetic tissues using monoclonal antibody to pyrraline. J Clin Invest 89: 1102–1112
18. Nishino T, Horii Y, Shiiki H, Yamamoto H, Makita Z, Bucala R, Dohi K (1995) Immunohistochemical detection of advanced glycosylation end products within the vascular lesions and glomeruli in diabetic nephropathy. Hum Pathol 26: 308–313
19. Yagihashi S, Kamijo M, Baba M, Yagihashi N, Nagai K (1992) Effect of aminoguanidine on functional and structural abnormalities in peripheral nerve of STZ-induced diabetic rats. Diabetes 41: 47–52
20. Vlassara H, Brownlee M, Cerami A (1981) Nonenzymatic glycosylation of peripheral nerve protein in diabetes mellitus. Proc Natl Acad Sci USA 78: 5190–5192
21. Vogt BW, Schleicher ED, Wieland OH (1982) e-Amino-lysine-bound glucose in human tissues obtained at autopsy. Increase in diabetes mellitus. Diabetes 31: 1123–1127
22. Horiuchi S, Araki N, Morino Y (1991) Immunochemical approach to characterize advanced glycation end products of Maillard reaction. J Biol Chem 266: 7329–7332
23. National Diabetes Data Group (1979) Classification and diagnosis of diabetes mellitus and other categories of glucose intolerance. Diabetes 28: 1039–1057
24. Vita G, Santoro M, Trombetta G, Leonardi L, Messina C (1992) A computer-assisted automatic method for

myelinated nerve fiber morphometry. Acta Neurol Scand 85: 18–22
25. Nitsch R, Klauer G (1989) Cryostat sections for coexistence studies and preembedding electron microscopic immunocytochemistry of central and peripheral nervous system tissue. Histochemistry 92: 459–465
26. Ribeiro-Da-Silva A, Priestley JV, Cuello AC (1993) Preembedding ultrastructual immunocytochemistry. In:Cuello AC (eds) Immunohistochemistry II. John Wiley & Sons, Chichester, pp181–227
27. Brownlee M (1992) Glycation products and the pathogenesis of diabetic complications. Diabetes Care 15: 1835–1843
28. Ikeda K, Higashi T, Sano H et al. (1996) Nε-(carboxymethyl)lysine protein adduct is a major immunological epitope in proteins modified with advanced glycation end products of the Maillard reaction. Biochemistry 35: 8075–8083
29. Ahmed MU, Thorpe SR, Baynes JW (1986) Identification of Nε-carboxymethyllysine as a degradation product of fructoselysine in glycated proteins. J Biol Chem 261: 4889–4894
30. Bucala R, Tracey KJ, Cerami A (1991) Advanced glycosylation products quench nitric oxide and mediate defective endothelium-dependent vasodilatation in experimental deabetes. J Clin Invest 87: 432–438
31. Kirstien M, Brett J, Radoff S, Ogawa S, Stern D, Vlassara H (1990) Advanced protein glycosylation induces transendothelial human monocyte chemotaxis and secretion of platelet-derived growth factor: role in vascular disease of diabetes and aging. Proc Natl Acad Sci USA 87: 9010–9014
32. Kirstein M, Aston C, Hintz R, Vlassara H (1992) Receptor-specific induction of insulin-like growth factor I in human monocytes by advanced glycosylation end product-modified proteins. J Clin Invest 90: 439–446
33. Olsson Y (1990) Microenvironment of the peripheral nervous system under normal and pathological conditions. Crit Rev Neurobiol 5: 265–311
34. Beamish NG, Stolinski C, Thomas PK, King RHM (1991) Freeze-fracture observations on normal and abnormal human perineurial tight junctions: alterations in diabetic polyneuropathy. Acta Neuropathol 81: 269–279
35. Williams SK, Howarth NL, Devenny JJ, Bitensky MW (1982) Structual and functional consequences of increased tubulin glycosylation in diabetes mellitus. Proc Natl Acad Sci USA 79: 6546–6550
36. Cullum NA, Mahon J, Stringer K, Mclean WG (1991) Glycation of rat sciatic nerve tubulin in experimental diabetic mellitus. Diabetologia 34: 387–389
37. Ryle C, Donaghy M (1994) Non-enzymatic glycation of peripheral nerve proteins in experimental diabetes mellitus. In: Peripheral Neuropathy Assoc (eds) Proceedings of PNS meeting. St. Paul, p.156 (Abstract)